Palmprint Classification Using Principal Lines

Abstract

This paper proposes a novel algorithm for the automatic classification of low-resolution palmprints. First we use some directional line detectors to extract the principal lines according to their characteristics and their definitions in two steps: the potential beginnings ("line initials") of the principal lines are extracted and then, on the basis of these line initials, a recursive process is applied to extract the principal lines in their entirety. Then palmprints are classified into six categories based on the number of the principal lines and the number of their intersections. The proposed algorithm has been shown to classify palmprints with an accuracy of 96.03%.

1. Introduction

A palm, which is the inner-surface of the hand between the wrist and the fingers [1], contains many features, such as palm shape, lines, ridges, and textures, etc. Palmprint is defined as the prints on a palm, which is mainly composed of the palm lines and ridges. Recently, palmprints, as an important complement of biometric characteristic, have been investigated extensively in automated personal authentication. Duta [2] employed palm lines for identity recognition. Zhang [3] extracted texture features from palmprints for the purposes of personal identification. Han [4] and Kumar [5] used the operator-based approach to extract the line-like features from palmprints for palmprint recognition.

All of these palmprint authentication methods require that the input palmprint should be matched against a large number of palmprints in a database, which is very time consuming. As fingerprint classification [6, 7], palmprint classification, which is a coarse-level matching of palmprint, can reduce the search time and computational complexity in palmprint recognition. Shu [8] used the orientation property of the ridges on palms to classify the offline high-resolution palmprints into six categories. Obviously, this classification method is unsuitable for low-resolution palmprints because it is difficult to obtain the orientation of the ridges from low-resolution images. As the first attempt for online low-resolution palmprint classification, we classify palmprints by using their most visible and stable features, i.e. the principal lines. Most palmprints show three principal lines: heart line, head line and life line (Figure 1 (a)). In this paper, we classify palmprints into six categories according to the number of principal lines and the number of their intersections.

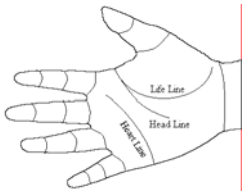

Figure 1. The typical principal lines on a palm

The rest of this paper is organized as follows. Section 2 presents some definitions and notation. In Section 3, some key points in palmprint are detected. Section 4 details how principal lines are extracted. Section 5 explains the criteria for palmprint classification. Section 6 gives some experimental results, and Section 7 provides some conclusions.

2. Definitions and Notation

Because there are many lines in palmprints, it is very difficult – without explicit definitions – to distinguish principal lines from mere wrinkles. When people discriminate between principal lines and wrinkles, the position and thickness of the lines play a key role. We, likewise, define the principal lines according to their positions and thickness.

To decide the positions of principal lines, we first define some points and straight lines in a palmprint. Figure 2 (a) illustrates these points and straight lines. Points A, B, C, F and G are the root points of the thumb, forefinger and little finger. Points D and E are the midpoints of the root line of the middle finger and the ring finger. Line BG is the line passing through Points B and G. Line AH is the straight line parallel with Line BG, intersecting with the palm boundary at Point H. Line AB is the line passing through Points A and B. Line CL is the straight line parallel with Line AB and intersecting with Lines BG and AH at Points M and L, respectively. Line GH passes through Points G and H. Lines FI and EJ are the straight lines parallel with Line GH and intersecting with Lines BG and

AH at Points P, I, J and O, respectively. K is the midpoint of straight line segment AH. Line DR passes through Points D and K. Line EQ is the straight line parallel with Line DR. It intersects with the palm boundary at Point Q.

Now, according to these defined points and lines, we define the principal lines as below:

The ***Heart line*** is a smooth curve that satisfies the following conditions (Figure 2 (b)):

1. Originating from Region GHIP;
2. Running across Line-segment OJ;
3. Not running across Line-segment AH.

The ***Head line*** is a smooth curve that satisfies the following conditions (Figure 2 (c)):

1. It is not the same curve as the extracted heart line;
2. Originating from Region ABML;
3. Running across Straight-line DR;
4. The straight line which passes the two endpoints of this curve runs across Line-segment EQ;
5. The straight line that passes the two endpoints of this curve does not run across Line-segment BG.

The ***Life line*** is a smooth curve that satisfies the following conditions (Figure 2 (d)):

1. Originating from Region ABML;
2. Running across Line-segment AH;
3. The straight line that passes the two endpoints of this curve does not run across Line-segment EQ.

In our work, we describe principal lines according to three basic rules. First, the number of each type of principal line occurring in a palmprint is not greater than 1. If there are more than one lines satisfying the same conditions, we keep the one with the greatest average thickness. Second, we do not consider broken principal lines. When a principal line is broken at some place, we regard the broken point as its endpoint. Third, we regard each principal line as a curve without branches. Thus, if there are branches, we keep the smoothest curve and discard the others.

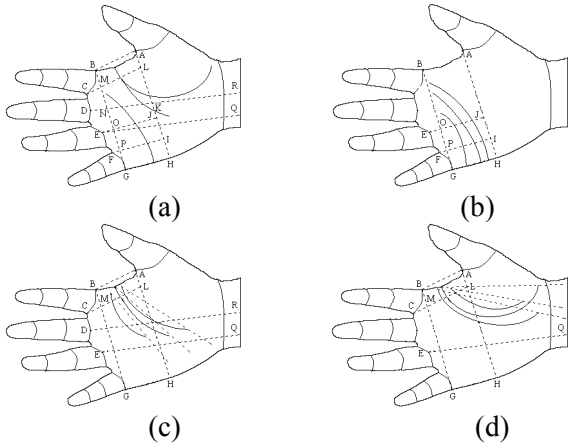

Figure 2. Definitions: (a) the defined points and lines on a palm, (b) the heart line, (c) the head line and (d) the life line.

3. Key points detection

According to the above definitions, before we can extract principal lines, we must first detect a set of points and lines. Point A, B, C, D, E, F and G are the key points from which the other points and the defined lines can be easily obtained according to their definitions (Figure 2 (a)). All images used in this paper were captured online using a CCD-camera-based device fitted with three pegs. One peg separates the first and middle fingers, another the middle and third fingers, and the final peg separates the third finger and little finger. These pegs are broad enough to stretch the fingers apart, thereby allowing us to detect the key points.

Detecting key points begins with extraction of the boundary of the palm by first smoothing the original image (Figure 3 (a)) using a low-pass filter and a threshold to convert it to a binary image and then tracing the boundary of the palm (Figure 3 (b)). In our database, a small portion of some palm images below the little finger is not captured. In these cases, we use the corresponding boundary segment of the image to represent the missing palm boundary segment.

Detecting Point A (Figure 3 (c)):

1. Find a point (X) on the thumb boundary;
2. Find the point (Y) on the palm boundary whose column index is less l than that of Point X (here, $l = 30$);
3. In all points on the palm boundary segment between Point X and Point Y, find the point which is farthest from Line XY as Point A.

Detecting Points C, D, E and F:

1. Use straight lines, L_1, L_2, L_3, L_4, L_5 and L_6, to fit the segments of the boundary of the forefinger, middle finger, third finger and little finger (Figure 3 (c));
2. Compute the bisectors (B_1, B_2 and B_3) of the angles formed by L_1 and L_2, L_3 and L_4, and L_5 and L_6. The intersections of B_1, B_2 and B_3 with palm boundary segments between the fingers are Point P_1, P_2 and P_3 (Figure 3 (c));
3. Find the points Q_1 and Q_2 on the boundary of forefinger and middle finger, whose column index is less l_1 than that of Point P_1 (here $l_1 = 30$), and link up P_1Q_1 and P_1Q_2 (Figure 3 (d));
4. In all points on the finger boundary segment between Point P_1 and Point Q_1, find the point which is farthest from Line P_1Q_1 as one root point of the forefinger, C (Figure 3 (d));
5. In all points on the finger boundary segment between Point P_1 and Point Q_2, find the point which is farthest from Line P_1Q_2 as one root point of the middle finger, T_1 (Figure 3 (d));
6. The root points of the middle finger, ring finger and little finger, T_2, T_3, T_4 and F, are obtained by using the same technique as described in 4~5 (Figure 3 (d));

7. Link up T_1T_2 and T_3T_4, and take their midpoints as Points D and E (Figure 3(e));

Detecting Points B and G (Figure 3 (e)):

1. Draw the perpendicular of Line L_2 from Point C, L_7, and intersect with palm boundary at Point B;
2. Draw the perpendicular of Line L_5 from Point G, L_8, and intersect with palm boundary at Point G.

Figure 3 (f) shows the palmprint overlaid with the obtained key points and the defined lines.

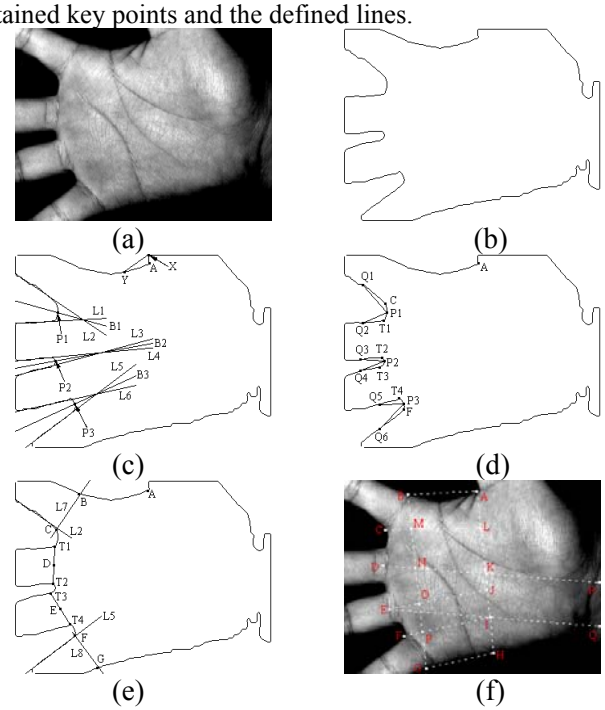

Figure 3. Detecting key points

4. Principal lines extraction

Palm-lines, including the principal lines and wrinkles, are a kind of roof edge. A roof edge is generally defined as a discontinuity in the first-order derivative of a gray-level profile [9]. In other words, the positions of roof edge points are the zero-cross points of their first-order derivatives. Moreover, the magnitude of the edge points' second-derivative can reflect the strength of these edge points [10]. In this paper, we compute the first-order derivative and the second-derivative in the vertical (90^0) direction by convolving the image with the following kernels:

$$H_1^0 = \begin{bmatrix} 0.0009 & 0.0027 & 0.0058 & 0.0092 & 0.0107 & 0.0092 & 0.0058 & 0.0027 & 0.0009 \\ 0.0065 & 0.0191 & 0.0412 & 0.0655 & 0.0764 & 0.0655 & 0.0412 & 0.0191 & 0.0065 \\ 0.0000 & 0.0000 & 0.0000 & 0.0000 & 0.0000 & 0.0000 & 0.0000 & 0.0000 & 0.0000 \\ -0.0065 & -0.0191 & -0.0412 & -0.0655 & -0.0764 & -0.0655 & -0.0412 & -0.0191 & -0.0065 \\ -0.0009 & -0.0027 & -0.0058 & -0.0092 & -0.0107 & -0.0092 & -0.0058 & -0.0027 & -0.0009 \end{bmatrix}$$

$$H_2^0 = \begin{bmatrix} 0.0156 & 0.0211 & 0.0309 & 0.0416 & 0.0464 & 0.0416 & 0.0309 & 0.0211 & 0.0156 \\ 0.0257 & 0.0510 & 0.0954 & 0.1441 & 0.1660 & 0.1441 & 0.0954 & 0.0510 & 0.0257 \\ -0.0298 & -0.1125 & -0.2582 & -0.4178 & -0.4896 & -0.4178 & -0.2582 & -0.1125 & -0.0298 \\ 0.0257 & 0.0510 & 0.0954 & 0.1441 & 0.1660 & 0.1441 & 0.0954 & 0.0510 & 0.0257 \\ 0.0156 & 0.0211 & 0.0309 & 0.0416 & 0.0464 & 0.0416 & 0.0309 & 0.0211 & 0.0156 \end{bmatrix}$$

The first-order derivative and the second-derivative in $\theta + 90^0$ direction can be computed by convolving the image with H_1^θ, H_2^θ, which are obtained by rotating H_1^0, H_2^0 with angle θ. H_1^θ, H_2^θ are called *directional line detectors* in θ direction. The position of the directional line points in θ direction can be obtained by looking for the zero-cross points of the first-order derivative in $\theta + 90^0$ direction. And the values of the corresponding points in the second-derivative are regarded as the magnitudes of the roof edge. Since all palm-lines are valleys, only the plus values in the second-derivative are kept. After thresholding, we can obtain the directional line in θ direction.

Given that the directions of principal lines are not constant, we apply suitable directional line detectors for principal line detection according to their local information.

The life and head lines are defined as originating from Region ABML and the heart line originates from Region GHIP (Figure 2). Therefore we can extract the beginnings ("line initials") of the principal lines from these regions and then use these initials as a basis to extract the principal lines in their entirety.

4.1. Extracting potential line initials of principal lines

A careful examination of a palmprint reveals that each principal line will initially run almost perpendicular to its neighboring palm boundary segment – approximated here by Line AB (life and head line) or Line GH (heart line) (Figure 3 (f)). If we denote the slope angle of the corresponding line (Line AB or Line GH) as θ, then the directions of the line initials of the principal lines are close to $\theta + 90^0$, so we first extract all lines in this region using the $\theta + 90^0$ line detectors $H_1^{\theta+90^0}, H_2^{\theta+90^0}$. Each of these extracted line segments is a potential line initial of principal lines. Hence, we should extract all of the lines whose line initials are the extracted line segments in these regions and keep the principal lines according to their definitions. Figure 4 shows these extracted lines: (a) is the original palmprint and (b) is the palmprint overlaid with the extracted potential line initials of the principal lines.

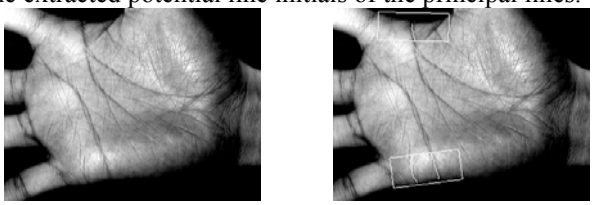

Figure 4. Potential line intials of the principal lines: (a) Original palmprint. (b) Palmprint overlaid with the extracted potential line initials of the principal lines.

4.2. Extracting heart lines

Because principal lines do not curve greatly, it is a simple matter to use the current extracted part of the line to predict the position and direction of the next short part. Now, based on the extracted potential line initials, we devise a recursive process to extract the whole heart line.

Suppose that Curve *ab* in Figure 5 (a) is the extracted part of the heart line of the palmprint shown in Figure 4. To extract the next part of the heart line, we trace back the extracted heart line *ab* from Point *b* and get the K^{th} point *c* (here K = 20). Since the heart line does not curve greatly, the region of interest (ROI), in which the next segment of heart line would be located, can be defined as a rectangular region $L \times W$ whose center point is Point *b*. Point *c* is the midpoint of one border whose length is *W*. *W* is a predefined value (here *W* = 20), and *L* is equal to twice the distance between Points *b* and *c* (Figure 5 (b)).

Joining Points *b* and *c* gives us straight line *cb*. The angle of the slope of straight line *cb* is α. Because principal lines curve so little, the direction of the next line segment should not vary much. Moreover, bearing in mind that the heart line may run to the bottom of the gap between forefinger and middle finger, i.e. the next line segment may turn δ degree ($45^0 > \delta > 0^0$) to the bottom of this gap (Figure 5 (b)), we employ directional line detectors H_1^{α}, H_2^{α} and $H_1^{\alpha+22.5^0}$, $H_2^{\alpha+22.5^0}$ to extract the line segment in this ROI, and then use logical "OR" to merge the lines in these two directions.

After processing the merged line image by closing and thinning, we keep all of the branches connecting with *ac* (Figure 5 (c)). If only one branch connected with *ac*, this branch is regarded as the next line segment. Otherwise, we choose one branch as follows. In Figure 5 (c), two branches, *cok* and *coh*, are connected with *ac* in ROI, where Point *o* is the branch point. Figure 5 (d) show the enlarged version of the ROI. We trace the line *oh*, *ok* and *oc* from Point *o* and get the N^{th} points *f*, *g* and *e*, respectively (here *N = 10*), and then link up *of*, *og* and *oe*, and compute Angle *foe* and Angle *goe*. The branch (*oh*) corresponding to the maximum angle is chosen as the next line segment.

After obtaining the next line segment, we should determine whether the heart line reaches its endpoint or not. We regard the heart line as having reached its endpoint if the line *ch* in the ROI satisfies one of the following two conditions:

If the minimum distance from endpoint *h to* three sides of the ROI (not including the side passing through Point *c*) exceeds a threshold T_d (here T_d = 5), Point *h* is the endpoint.

If Angle *cmh* is less than a threshold T_a (here $T_\alpha = 135^0$), having joined Points *c* and *h*, having supposed that Point *m* is the farthest point to the straight line *ch* on curve *ch*, and having joined *cm* and *hm*, Point *m* is the endpoint (Figure 5 (e)).

If the curve *ch* satisfies none of these conditions, we take the longer curve *ah* as the current extracted heart line and repeat this process recursively until the extracted curve reaches its endpoint.

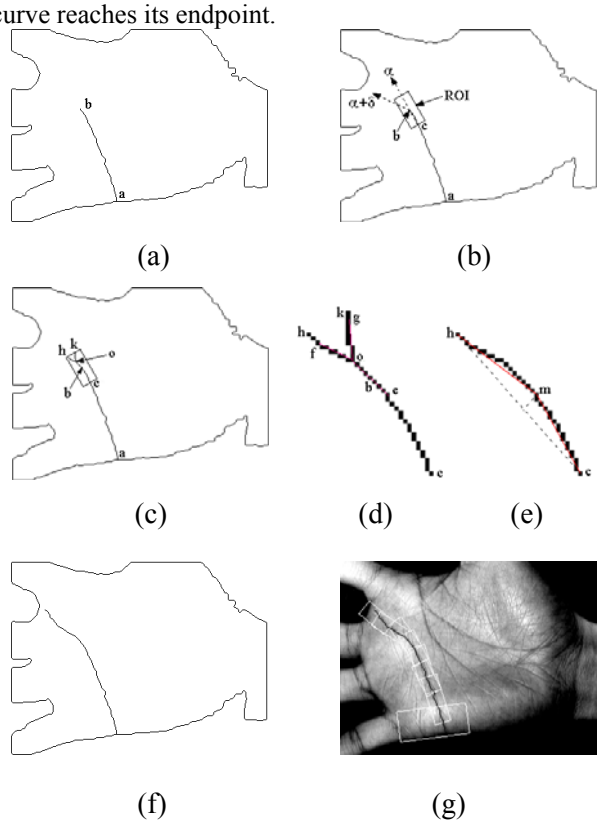

Figure 5. Extracting the heart line

The palmprint shown in Figure 4 had two lines extracted that originated from Region GHIP. According to the definition, only one of them is the heart line. Figure 5 (f) shows the whole extracted heart line and (g) is the palmprint overlaid with the whole heart line and all of the ROIs involved in this heart line extraction.

4.3. Extracting life and head lines

The processes of life line and head line extraction differs little from that of heart line extraction. One area of difference is in the rule that only one line may be extracted according to each line initial. While this works well in heart line extraction, it is not suitable for life and head line extraction because life and head lines may share their line initials. Given this, we apply our observation that the branch point of the life and head lines should not exceed Line-segment NK and LK (Figure 2). With this in mind, when using the recursive heart line extraction process to extract the life line and head line, if the extracted

curve does not run across Line-segment NK and LK and if there exists more than one branch, instead of choosing just one of the branches, we extract and trace the curves based on each branch. If the extracted curve crosses Line-segment NK or LK, the extraction process is the same as for heart line extraction.

Figure 6 illustrates the process of life and head line extraction: (a) is the extracted line including two branches. In the original heart line extraction process, only one branch (*oe*) would be kept and the other one (*of*) would be discarded. Obviously, it is wrong to discard branch *of* because it is a part of the life line. Since the extracted line does not run across Line-segment NK and LK, we split this branched curve into two curves *aoe* and *aof* (Figure 6 (b) and (c)) and extract the lines according to each of them. In this figure, the extracted curve related with *aoe* is the head line (Figure 6 (d)) and the one related with *aof* is the life line (Figure 6 (e)). Figure 6 (f) shows the palmprint overlaid with all of the extracted principal lines.

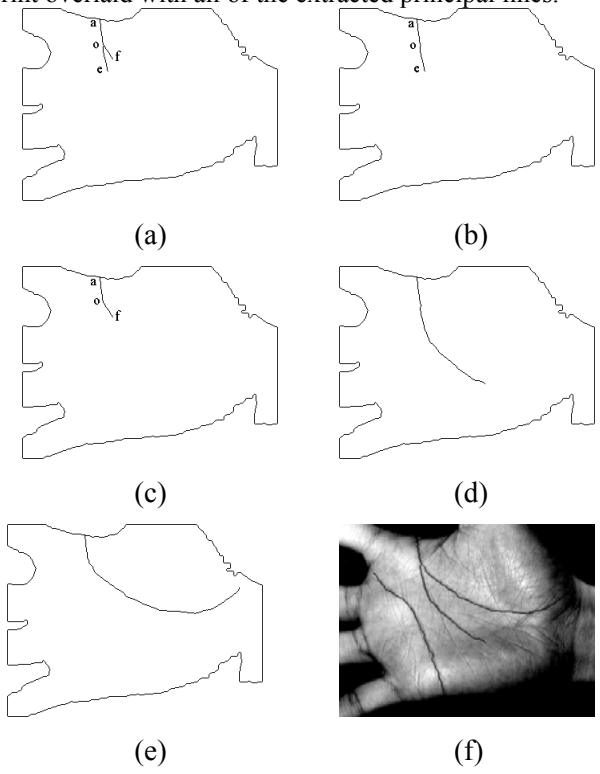

Figure 6. Extracting the life line and head line

5. Palmprint classification

We classify the palmprint by the number of the principal lines and the number of the intersections of these principal lines. There are at most three principal lines as the number of each type of principal line is not more than 1. Two principal lines are said to intersect if and only if some of their points overlap or some points of one line are the neighbors of some points of another line. If any two principal lines intersect, the number of intersections increases by 1. Therefore, the number of intersections of three principal lines is less than or equal to 3.

According to the number of their principal lines and the number of the intersections of these lines, palmprints can be classified into following six categories (Table 1):

Category 1: Palmprints composed of not more than one principal line (Figure 7 (a));

Category 2: Palmprints composed of two principal lines and no intersection (Figure 7 (b));

Category 3: Palmprints composed of two principal lines and one intersection (Figure 7 (c));

Category 4: Palmprints composed of three principal lines and no intersection (Figure 7 (d));

Category 5: Palmprints composed of three principal lines and one intersection (Figure 7 (e));

Category 6: Palmprints composed of three principal lines and more than one intersection (Figure 7 (f))

Table 1. Palmprint classification rules

Number of Principal Lines	≤1	2		3		
Number of the Intersections of Principal Lines	0	0	1	0	1	≥2
Category No.	1	2	3	4	5	6

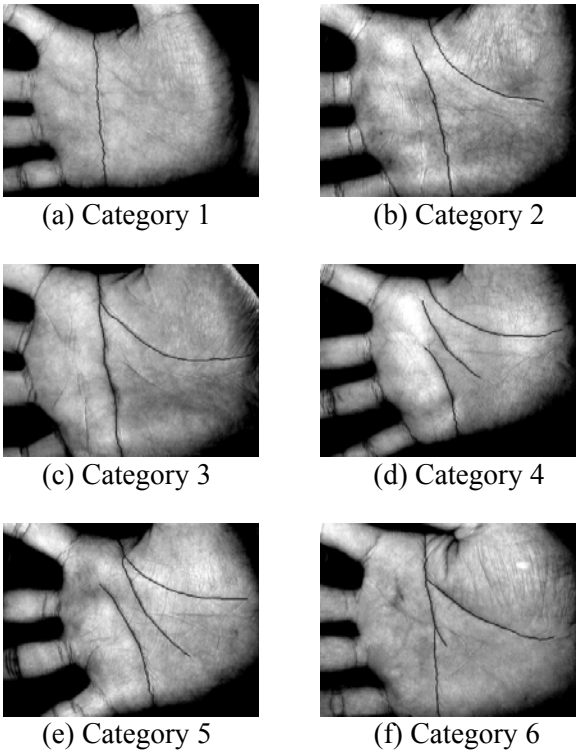

Figure 7. Examples of each palmprint category

6. Experimental results

Our palmprint classification algorithm was tested on a database containing 13,800 palmprints captured from 1,380 different palms using a CCD-camera-based device, 10 images per palm. The images are 320 × 240 and the palmprints have been labeled manually. In this database, 0.36% samples belong to Category 1, 1.23% to Category 2, 2.83% to Category 3, 11.81% to Category 4, 78.12% to Category 5 and 5.65% to Category 6. The Hysteresis threshold method [11] was used in which the threshold is obtained automatically by using Otsu's method [12].

Correct classification takes place when the palmprint is classified into a category which has the same label with this palmprint. Misclassification takes place when the palmprint is classified into a category whose label is not same with the label of this palmprint. In all of the 13,800 palmprints in the database, 548 samples were misclassified: 7 in Category 1, 11 in Category 2, 25 in Category 3, 104 in Category 4, 349 in Category 5 and 47 in Category 6. Most of the misclassification can be attributed to images of poor quality. The classification accuracy is about 96.03%. The confusion matrix is given in Table 3 and the classification accuracy in Table 4.

7. Conclusion

As the first attempt to classify low-resolution palmprints, this paper presents a novel algorithm for palmprint classification using principal lines. The potential line initials of the principal lines are firstly extracted by using directional line detectors and then the principal lines are extracted in their entirety using a recursive process. The palmprints are classified into six categories according to the number of the principal lines and their intersections. According to the statistical results from our database containing 13,800 palmprints, the distributions of Categories 1~6 are 0.36%, 1.23%, 2.83%, 11.81%, 78.12% and 5.65%, respectively. The proposed algorithm classified these palmprints with 96.03% accuracy.

Table 2. Distribution of each category in our database

Category NO.	1	2	3	4	5	6
Number of Palmprints	50	170	390	1,630	10,780	780
Percent (%)	0.36	1.23	2.83	11.81	78.12	5.65

Table 3. Classification results of the proposed algorithm

Assigned Category NO.	True Category NO.					
	1	2	3	4	5	6
1	**43**	6	3	23	41	2
2	3	**159**	1	41	132	7
3	4	0	**365**	18	95	13
4	0	3	2	**1,526**	12	0
5	0	2	11	13	**10,431**	25
6	0	0	8	9	69	**733**

Table 4. Classification accuracy of the proposed algorithm

Total Samples	Correctly Classified Samples	Misclassified Samples	Classification Accuracy
13,800	13,252	548	96.03%

References

[1] D. Zhang, Automated Biometrics – Technologies and Systems, Kluwer Academic Publishers, 2000.

[2] N. Duta, A.K. Jain, and K.V. Mardia, "Matching of palmprint," Pattern Recognition Letters, vol. 23, no. 4, pp. 477-485, 2001.

[3] D. Zhang, W. Kong, J. You and M. Wong, "Online palmprint identification," IEEE Transactions on Pattern Analysis and Machine Intelligence, vol. 25, no. 9, pp. 1041-1050, 2003.

[4] C. C Han, H. L. Chen, C. L. Lin and K. C. Fan, "Personal authentication using palm-print features," Pattern Recognition, vol. 36, no. 2, pp. 371-381, 2003.

[5] A. Kumar, D. C. M. Wong1, H. C. Shen1, A. Jain, "Personal Verification using Palmprint and Hand Geometry Biometric," Lecture Notes in Computer Science, vol. 2688, pp. 668-678, 2003.

[6] K. Karu and A. K. Jain, "Fingerprint Classification," Pattern Recognition, vol. 29, no. 3, pp. 389-404, 1996.

[7] R. ppelli, A.Lumini, D. Maio and D. Maltoni, "Fingerprint Classification by Directional Image Partitioning," IEEE Transactions on Pattern Analysis and Machine Intelligence, vol. 21, no. 5, pp. 402-421, 1999.

[8] W. Shu, G. Rong and Z. Bian, "Automatic palmprint verification," International Journal of Image and Graphics, vol. 1, no. 1, pp. 135-151, 2001.

[9] R. M. Haralick, "Ridges and Valleys on Digital Images," Computer Vision, Graphics, and Image Processing, vol. 22, pp. 28-38, 1983.

[10] K. Liang, T. Tjahjadi and Y. Yang, "Roof edge detection using regularized cubic B-spline fitting," Pattern Recognition, vol. 30, no. 5, pp. 719-728, 1997.

[11] J. Canny, "A computational approach to edge detection," IEEE Transactions on Pattern Analysis and Machine Intelligence, vol. 8, no. 6, pp. 679-698, 1986.

[12] J. R. Parker, Algorithms for Image Processing and Computer Vision, John Wiley & Sons, Inc., 1997.